Talanta 79 (2009) 1322–1330

Contents lists available at ScienceDirect

Talanta

journal homepage: www.elsevier.com/locate/talanta

Precipitation as a simple and versatile method for preparation of optical nanochemosensors

Sergey M. Borisov*, Torsten Mayr, Günter Mistlberger, Kerstin Waich, Klaus Koren, Pavel Chojnacki, Ingo Klimant

Institute of Analytical Chemistry and Food Chemistry, Graz University of Technology, Stremayrgasse 16, 8010 Graz, Austria

ARTICLE INFO

Article history:
Received 23 March 2009
Received in revised form 13 May 2009
Accepted 26 May 2009
Available online 6 June 2009

Keywords:
Nanosensor
Luminescence
Precipitation
Polymer

ABSTRACT

Optical nanosensors for such important analytes as oxygen, pH, temperature, etc. are manufactured in a simple way via precipitation. Lipophilic indicators are entrapped into nanobeads based on poly(methyl methacrylate), polystyrene, polyurethanes, ethylcellulose, and other polymers. Charged groups greatly facilitate formation of the small beads and increase their stability. Sensing properties of the beads can be tuned by choosing the appropriate indicator. Nanosensors for carbon dioxide and ammonia are found to be cross-sensitive to pH if dispersed in aqueous media. These nanobeads are successfully employed to design bulk optodes. Nanochemosensors with enhanced brightness via light-harvesting and multi-functional magnetic nanosensors also are prepared.

1. Introduction

Such important analytes as oxygen, pH, ions, etc. are nowadays routinely monitored with the help of optical sensors. A large group of optical sensors relies on the use of indicators which respond to the species of interest by altering their luminescent properties (intensity and decay time) and, therefore, allow for contactless measurements. Luminescent chemosensors are commonly used in several widespread formats such as planar sensor foils [1,2] and spots [3], paints [4–6], fiber-optic (micro)sensors [7–9] and nanosensors [10,11]. Optical nanosensors became increasingly popular in the last decade [12]. They represent versatile analytical tools that combine the flexibility of the dissolved indicators (small size, suitability for imaging in volume) with the robustness of the bulk optodes (high selectivity, low interferences). Despite that the nanosensors are commonly used for measurements in aqueous media, the beads also can be dispersed in polymer matrices. Particularly, multi-analyte sensing becomes possible if several kinds of beads are mixed together [13,14]. Thus, preparation of analyte-sensitive nanobeads with desired properties is of much practical interest. Some nanosensors reported recently rely on quantum dots [15], metal beads [16] and other materials; however, most of the nanosensors make use of indicators embedded in polymer beads and sol–gels [17,18]. This approach enables rapid technology transfer since bulk optodes for different analytes are well established. Several major staining techniques can be distinguished for polymeric beads. First, an indicator can be added into the mixture of monomers to be entrapped in the bead during polymerization [19,20]. Both physical entrapment and covalent coupling are used. Staining of polymeric beads by swelling is another common method [21]. Finally, dyed polymer beads can be obtained by solvent displacement method (precipitation) [22,23]. Despite the fact that undoped polymeric beads are often produced via precipitation [24–26], this method was only sparsely used for preparation of optical nanochemosensors [27]. However, it has high potential due to simplicity and versatility, but also due to the fact that no surfactants (which affect biological systems) are required for preparation of the beads. In this contribution we report strategies for making nanochemosensors by precipitation and provide examples of nanobeads sensitive to oxygen, pH and other important analytes.

2. Experimental

2.1. Materials

Poly(styrene-co-maleic anhydride) (PS-MA; 7% of maleic anhydride; MW 224,000), polysulfone (PSulf, MW 26,000), N,N′-dimethyl-9,9′-biacridinium dinitrate (lucigenin), cellulose acetate (MW 100,000; CAc), cellulose acetate propionate (MW 15,000; CAcP), cellulose acetate butyrate with 44–48% butyrate content (CAcB) were obtained from Aldrich (www.sigmaaldrich.com). Poly(vinylidene chloride-co-acrylonitrile) (PViCl-PAN; 20 wt.%

* Corresponding author. Tel.: +43 316 873 4326; fax: +43 316 873 4329.
E-mail address: sergey.borisov@tugraz.at (S.M. Borisov).

0039-9140/$ – see front matter © 2009 Elsevier B.V. All rights reserved.
doi:10.1016/j.talanta.2009.05.041

polyacrylonitrile, MW 150,000), poly(methyl methacrylate-co-methacrylic acid) (PMMA-MA; 10% methacrylic acid, MW ~100,000), poly(2-hydroxyethyl methacrylate) (pHEMA, MW ~200,000) were from Polysciences (www.polysciences.com). Polyurethane hydrogels D4, D7 and hydrothan H15 were obtained from Cardiotech (www.cardiotech-inc.com). Ethylcellulose (EC, ethoxy content 46%), Nafion® 117 Solution (5% in alcohols) and tetraoctylammonium hydroxide (20% in methanol) were from Fluka (www.sigmaaldrich.com). Eudragit®RL 100 (~10% of quaternary ammonium groups, MW ~150,000) and Eudragit®RS 100 (~5% of quaternary ammonium groups, MW ~150,000) were purchased from Degussa. Tetrahydrofurane (THF), dimethylformamide (DMF) and acetone were obtained from Roth (www.carl-roth.de). Platinum(II) *meso*(2,3,4,5,6-pentafluoro)phenyl porphyrin (PtTFPP) was bought from Frontier Scientific (www.frontiersci.com). Nitrogen, oxygen and synthetic air (all of 99.999% purity) were obtained from Air Liquide (www.airliquide.at).

Fluorescein octadecylester (FODE) was synthesized according to the literature procedures [28,29]. 2′,7′-Dichlorofluorescein methylester (DCFME) was prepared as previously reported [27].

Preparation of the iridium(III) acetylacetonato-bis(3-(benzothiazol-2-yl)-7-(diethylamino)-coumarin) ($Ir(C_S)_2(acac)$) is reported elsewhere [30]. Palladium(II) tetraphenyltetrabenzoporphyrin (PdTPTBP) was prepared according to Finikova et al. [31]. The europium(III) complex $Eu(tta)_3$DEADIT was synthesized as described previously [32].

The chemical structures of the indicators and polymers used are shown in Fig. 1. Note that hydrogels D4, D7 and hydrothan H15 represent polyurethane-based block copolymers which possess hydrophilic and hydrophobic parts, however the exact composition is not available from the manufacture.

2.1.1. Preparation of the oxygen-sensitive and pH-sensitive beads via fast precipitation

Thirty milligrams of a polymer were dissolved in 15 g of a respective solvent (0.2%, w/w solution). The dye concentration (1%, w/w for $Ir(C_S)_2(acac)$, PdTPTBP; 0.25% (w/w) for FODE in respect to polymer) was adjusted using stock solutions. Then, 50 mL of water was added to the solution (~10 mL per second) under vigorous stirring. The solvents (THF, acetone) were removed under reduced pressure. Alternatively, DMF was removed by dialysis against water for 5 days using a regenerated cellulose dialysis membrane from Roth (MWCO 12,000–14,000).

2.1.2. Preparation of the chloride-sensitive beads

One gram of the Nafion® 117 Solution (50 mg of the polymer) was diluted with 10 mL of ethanol. Then, 2 mg of lucigenin in 10 mL of EtOH was added dropwise to the polymer solution. After 30 min of stirring 40 mL of water was added under vigorous stirring. 300 mg of NaF was added and the dispersion of the beads was stirred for 3 h. The excess of the dye, NaF and EtOH were removed by dialysis against water.

2.1.3. Preparation of the temperature-sensitive and DLR-reference nanobeads

Four hundred milligrams of PViCl-PAN and 6 mg of $Eu(tta)_3$DEADIT (for the temperature-sensitive beads) or 6 mg of $Ir(C_S)_2(acac)$ (for the DLR-reference beads) were dissolved in 200 mL of acetone. 600 mL of water was added dropwise under vigorous stirring. Acetone was removed under reduced pressure.

2.1.4. Preparation of the ammonia-sensitive beads

Ten milliliters of acetone containing 0.14 mg of DCFME and 100 mg of a cellulose ester (CAc, CAcP or CAcB) were added drop-wise into an ultra-sonicated round-bottomed flask containing 50 mL of Millipore water. The resulting nanobeads were dialysed against water for 24 h and freeze-dried. An NH_3-sensing membrane was prepared by dispersing the nanobeads in a silicone layer as described previously [27].

2.1.5. Preparation of the magnetic beads

44.5 mg of PS-MA, 0.44 mg $Ir(C_s)_2(acac)$ and 8.9 mg of magnetite (EMG1300, Ferrotec GmbH, www.ferrotec.com) were dissolved and dispersed, respectively, in 5 mL of tetrahydrofuran. This cocktail was mixed with 15 mL of water under vortexing, resulting in a suspension of swollen nanoparticles. After evaporation of THF under a slight air stream, the particles were magnetically collected and washed with deionized water. The washing was repeated twice and the beads containing no or little magnetite were discarded.

2.2. Measurements

The size of the beads and *Z* potential were determined with a particle size analyzer Zetasizer Nano ZS (www.malvern.de). Luminescence excitation and emission spectra were acquired on a Hitachi F-7000 fluorescence spectrometer (www.inula.at) equipped with a red-sensitive photomultiplier R 928 from Hamamatsu (www.hamamatsu.com). In the case of the pH nanosensors the pH was adjusted to the desired value using phosphate and phosphate-citrate buffers. The pH of the buffer solutions was controlled by a digital pH meter (InoLab pH/ion, WTW GmbH & Co. KG, www.wtw.com) calibrated at 20 ± 2 °C with standard buffers of pH 7.0 and 4.0 (WTW GmbH & Co. KG). The buffers were adjusted to constant ionic strength using sodium chloride as the background electrolyte.

Luminescence phase shifts were measured with a two-phase lock-in amplifier (SR830, Stanford Research Inc., www.thinksrs.com). The dispersion of the beads in water (~0.5 mg mL^{-1}) was placed in a glass vial and excited with sinusoidally modulated LED light. A bifurcated fiber bundle was used to guide the excitation light to the vial and to guide back the luminescence to a photomultiplier tube (H5701-02, Hamamatsu, www.sales.hamamatsu.com). The $Ir(C_S)_2(acac)$-based beads were excited with a 470 nm LED (www.roithner-laser.com), modulated at 20 kHz, while a 425 nm LED was used for the excitation of beads stained with PdTPTBP (f = 800 Hz) and $Eu(tta)_3$DEADIT (f = 700 Hz). In all cases, the excitation light was filtered though a BG 12 filter from Schott (www.schott.com). An OG 550 filter (Schott) was used for $Ir(C_S)_2(acac)$ and $Eu(tta)_3$DEADIT, and an RG 9 filter for PdTPTBP. Temperature was controlled by a cryostat ThermoHaake DC50. In the case of the oxygen-sensitive beads the temperature was kept constant at 25 °C. Gas calibration mixtures were obtained using a gas mixing device (MKS, www.mksinst.com). Three independent measurements were performed to obtain a calibration curve.

SEM images were acquired on a Zeiss Ultra 55 (www.smt.zeiss.com) equipped with a field emission gun. A drop of bead dispersion was placed on a polymeric substrate. After evaporation of water the samples were coated with a Ag–Pd layer (~10 nm) to avoid specimen charging.

Photographic images of the magnetic optical sensor particles were acquired using a Canon 5D color camera equipped with a 24–105 mm f/4L IS objective from Canon. Excitation of the beads was performed with a 366-nm line of a mercury lamp.

3. Results and discussion

3.1. General strategies

These are schematically shown in Fig. 2. Preparation of the sensing beads via precipitation relies on the use of two miscible solvents. Several key steps can be distinguished and include: (1) preparation of the sensor „cocktail"; (2) precipitation of the beads; and

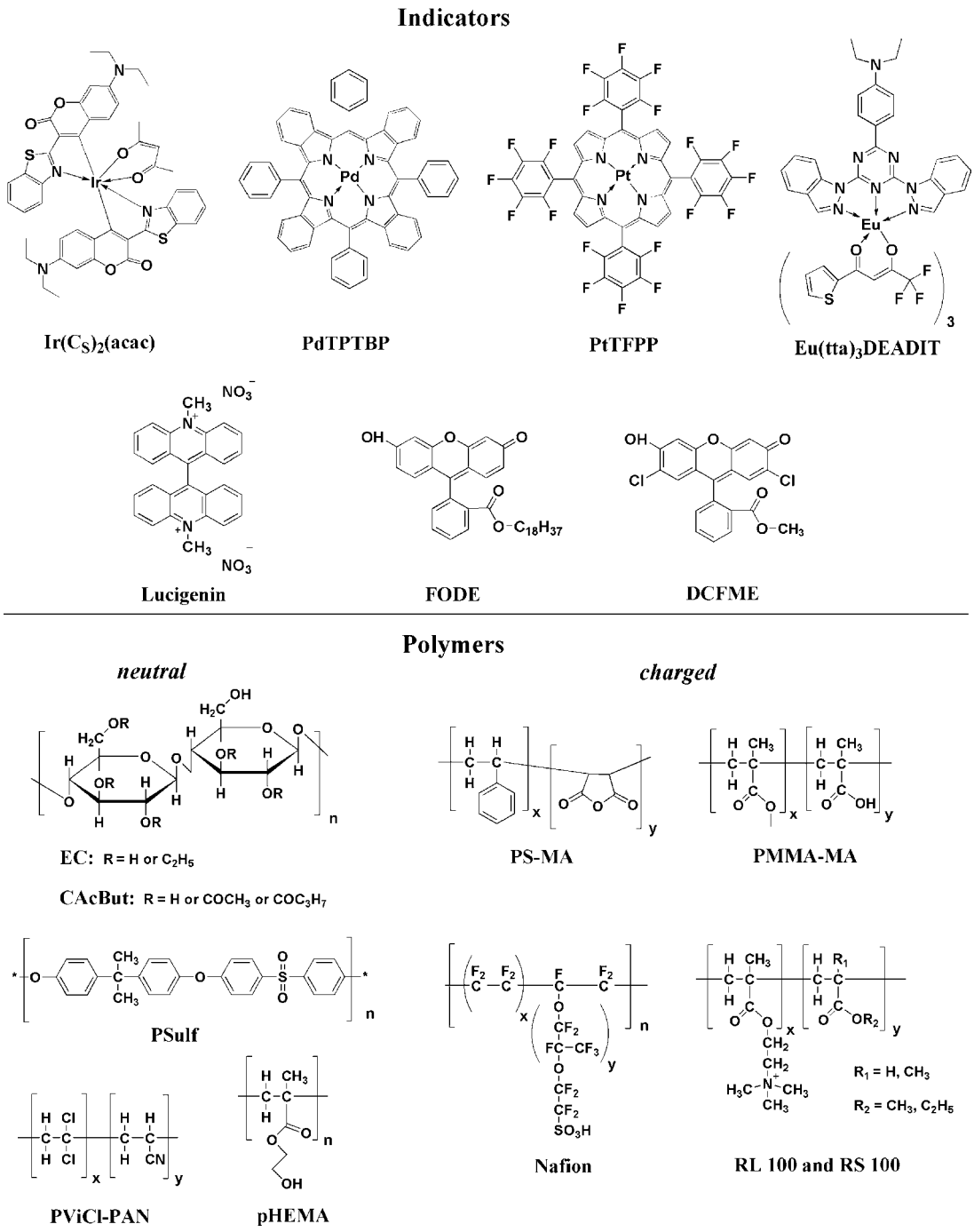

Fig. 1. Chemical structures of the indicators and polymers.

(3) removing of the organic solvent and purification. Strategies and trends will be discussed in the following.

3.1.1. Preparation of the sensor "cocktail"

The sensor "cocktail" is prepared by dissolving an indicator and a polymer in an organic solvent or in a mixture of several solvents. Notably, moderate solubilities of the components are sufficient, and typical concentrations required are 0.1–0.4% (w/w) for the polymer and 0.001–0.004% w/w for the indicator. This is in contrast to the bulk optodes which are prepared from more concentrated solutions (usually containing 5–10% (w/w) of the polymer and 0.02–0.2% of the indicator). A typical example includes encapsulation of the iridium(III) coumarin complex $Ir(C_S)_2(acac)$ into gas blocking PViCl-PAN. The polymer is excellently soluble in acetone; on the contrary, the dye is poorly soluble there. However, the solubility is sufficient for preparation of the sensor particles since only 3 mg of the dye is used per 100 mL of the solvent.

It should be mentioned that the size of the nanobeads can be adjusted by varying the concentration of the "cocktail". As can be seen from Table 1, the diluted solutions favor the formation of smaller beads.

3.1.2. Precipitation

The nanobeads are formed by diluting the solution with a "bad" solvent. It should be emphasized that this process does not require the addition of surfactants (and their subsequent removal) as in

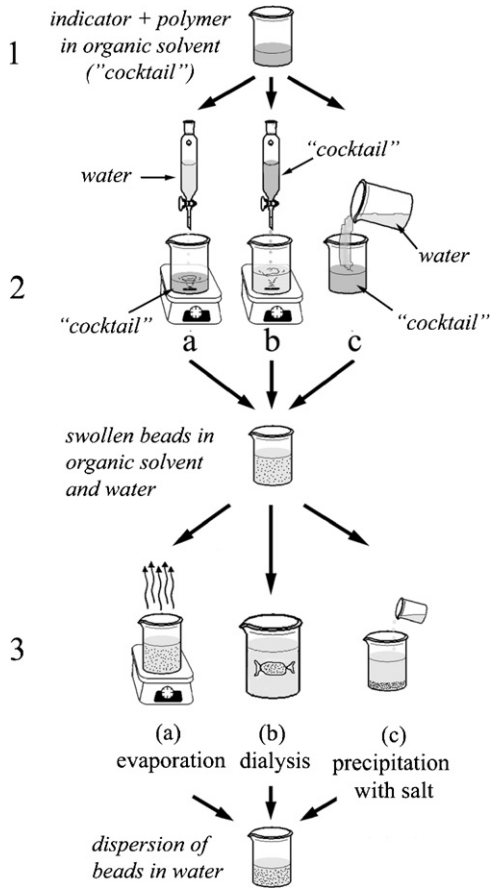

Fig. 2. Preparation of the nanosensors via precipitation: (1) preparation of the "cocktail" by dissolving indicator and polymer in organic solvent; (2) precipitating the particles ((a) slow addition of water into the "cocktail"; (b) slow addition of the "cocktail" in water; (c) fast mixing of the "cocktail" and water); (3) removing the organic solvent.

the case of nanosensors prepared via polymerization. Water is a solvent of choice in most cases since the nanosensors usually are designed for measurements in aqueous medium. Therefore, the use of lipophilic indicators (completely insoluble in water) is essential to ensure that no leaching from the nanoparticles will occur. It is also important that the indicator has good solubility in the polymer but both are poorly soluble in solvent:water mixtures. Otherwise, the indicator can aggregate and precipitate before the formation of beads or still remain in solution after polymeric beads are formed.

Table 1
Properties of the PS-MA nanobeads obtained via precipitation with water.

Organic solvent	Method	C polymer, % w/w	Z_{av}, nm	PDI
THF	2c + 3a	1	191	0.106
THF	2c + 3a	0.5	167	0.053
THF	2c + 3a	0.2	156	0.131
THF	2c + 3a	0.1	150	0.119
THF	2c + 3a	0.05	155	0.138
THF	2a + 3a	0.2	360	0.039
DMF	2a + 3c	0.2	240	0.092
THF:acetone (1:1)	2c + 3a	0.1	112	0.112
THF:acetone (1:3)	2c + 3a	0.1	94	0.071
THF:acetone (1:7)	2c + 3a	0.2	89	0.132

Suitable solvents for dissolving the polymers and indicators include dimethylformamide, dimethylsulfoxide, acetone, tetrahydrofuran, 1,4-dioxan, acetonitrile, ethanol, etc. These solvents can be as well mixed together to adjust solubility of polymers and indicators.

Three different strategies of precipitation can be used (Fig. 2): First, water can be slowly added under vigorous stirring to the "cocktail" (2a). Second, the "cocktail" can slowly be added to water (2b). Third, both water and the "cocktail" can be rapidly mixed together (2c). Usually, fast precipitation results in formation of smaller beads than if water is added slowly (Table 1). For example, in case of PS-MA beads precipitated from THF the size was found to be ~360 and ~150 nm, respectively for slow and fast water additions. The size of the beads also depends on the solvent used (Table 1). It was found that substitution of THF by acetone in case of PS-MA favors the formation of even smaller beads (Z_{av} < 100 nm). For certain polymers (such as polyacrylonitrile) slow precipitation also can result in formation of very small beads [22].

As we have found, a variety of the polymers can be used to prepare nanosensors (Table 2). It should be mentioned that polar groups present in the polymer facilitate bead formation and usually render particles stable in water. Therefore, such polar polymers as ethylcellulose, polysulfone, polyurethanes and polyacrylonitriles can be polymers of choice. The resulting beads are stable in water and do not show aggregation. However, the nanobeads often aggregate readily in the presence of salts (Table 2). Obviously, small amount of charged groups (e.g. carboxyl groups) can greatly increase bead stability in water. Such copolymers as PS-MA or PMMA-MA were found to be excellently suitable for preparation of the nanosensors. The nanobeads do not aggregate even at high salt concentration, can be freeze-dried and redispersed easily. Surprisingly, positively charged Eudragits RL 100 and RS 100 (which contain quaternary ammonium groups) show much higher tendency to aggregation even at physiological ionic strength (150 mM).

Table 2
Properties of the polymeric nanobeads obtained via precipitation with water.

Polymer	Organic solvent	C polymer, % w/w	Method	Z_{av}, nm	PDI	Z potential, mV	Freeze-drying[a]	Aggregation in 150 mM NaCl[b]
PS-MA	THF:acetone 1:3	0.2	2c + 3a	94	0.071	−41	+	–
PMMA-MA	THF:acetone 1:9	0.2	2c + 3a	55	0.082	−36	+	–
RL-100	Acetone	0.2	2c + 3a	45	0.200	+58	+	+
RS-100	Acetone	0.2	2c + 3a	44	0.188	+48	+	+
EC	THF:acetone 1:1	0.2	2c + 3a	72	0.089	−27	+	+
PViCl-PAN	THF:acetone 1:9	0.2	2c + 3a	53	0.092	−28	+	+
PSulf	THF:acetone 1:1	0.2	2c + 3a	432	0.031	−23	+	+
D4	DMF	0.4	2c + 3c	220	0.060	−7.8	–	–
D7	DMF	0.4	2c + 3c	250	0.103	−6.0	–	–
H15	DMF	0.4	2c + 3c	515	0.046	−7.6	–	–
pHEMA	DMF	0.4	2c + 3c	152	0.187	−31	–	+
Cel Ac But	Acetone	1	2b + 3b	150	0.120	Not determined	+	+
Nafion	Ethanol	0.5	2c + 3c	220[c]	–	Not determined[c]	+	–

[a] –not redispersible; +redispersible.
[b] Size of the aggregates >1 μm; bead concentration is 0.5 mg/mL.
[c] Size and Z potential cannot be determined since the beads are not scattering; the size determined by scanning electron microscopy.

It should be mentioned that this methodology can also be used for preparation of nanobeads from apolar polymers such as e.g. polystyrene. Although these nanobeads cannot be used for sensing purposes in aqueous media, they are suitable as components of composite materials such as, for example, multi-analyte sensors. Precipitation of the nanobeads is to be performed with a second organic solvent in which both the indicator and the polymer are not soluble. Suitable candidates include such polar solvents as ethanol or methanol or, alternatively, apolar hexane. Most polymers and lipophilic indicators are poorly soluble in these solvents and thus can be precipitated. For example, stained polystyrene beads were obtained by dissolving the polymer and the dye in dichloromethane and precipitating the particles with hexane.

3.1.3. Purification of the beads

Here, an organic solvent is removed. If the boiling point of this solvent is lower than that of water, it can be removed at elevated temperatures under reduced pressure, or even by bubbling air or nitrogen through (3a). If the boiling point of the organic solvent is higher (DMF, DMSO) two strategies are possible. The beads can be precipitated with help of sodium chloride, separated by centrifugation and washed with water several times. This method was found useful for purification of PAN nanoparticles [22]. Alternatively, dialysis can be used but is rather time consuming. We used dialysis to purify nanosensors based on hydrogels D4, D7, hydrothan H15 and pHEMA since the beads were found to irreversibly aggregate after precipitation with NaCl and subsequent centrifugation. It should also be mentioned that if a polymer is not swellable in ethanol or methanol, these solvents can be used to wash the particles after precipitation. This helps to remove the indicator molecules adsorbed on the surface.

3.2. Properties of the polymeric nanobeads

Table 2 gives an overview of the polymeric beads investigated. Evidently, a variety of polymers can be used to prepare beads which differ significantly in their properties. As can be seen, the polymers bearing positively or negatively charged groups can be used to prepare rather small nanobeads (Z_{av} < 100 nm). On the other side, neutral polymers such as hydrogels form much bigger beads. If similar polymers are used (e.g. those based on polyurethanes) the size of the beads is likely to increase with decreasing polarity. In fact, Z_{av} was found to be 220, 250 and 515 nm for D4, D7 and H15, respectively. According to the manufacture, the water uptake by these polymers is 51%, 30% and 15%, respectively.

The morphology of the nanoparticles was investigated by scanning electron microscopy. The size of the beads estimated from the SEM images (Fig. S1–S7) is in a good agreement with the data obtained in light scattering experiments. For example, the average diameter of the beads based on PMMA-MA, EC, PViCl-PAN and PS-MA (precipitated from THF) was estimated to be 62 ± 9, 63 ± 6, 39 ± 8 and 155 ± 40 nm, respectively. In contrast to other polymeric beads that appear to be spherical, the Nafion particles are not symmetrical (Fig. S5) and are very polydisperse (220 ± 80 nm). It can also be observed that the hydrogel D4 beads shrank dramatically upon drying so that the size is reduced ~70 nm. Unfortunately, the RS-100 and RL-100 beads formed a dense layer upon drying so that no beads can be distinguished.

A quite important property of the beads is their tendency to aggregate in the presence of electrolytes and/or other substances such as e.g. proteins. Some of the beads were found to aggregate readily at physiological ionic strength (Table 2). Due to aggregation, these beads also are rather poorly suitable for use in cultivation media, such as an LB medium. These contain significant amount of salts, but also proteins. Since aggregation is concentration-dependent the nanobeads are likely to be still useful at lower concentrations, providing that the brightness of the beads is sufficient for measurements (such as for the beads stained with an ultra-bright $Ir(C_s)_2(acac)$). In fact, if the concentration of beads is reduced to 0.25 mg/mL, micrometer-sized aggregates do not form in case of EC and the hydrogels, and the RL-100 nanobeads are apparently not affected at this concentration. As expected, the RL-100 beads which are more positively charged than the chemically similar RS-100 particles are also more resistant to aggregation. On the other side, the nanobeads based on PViCl-PAN, RS-100 and pHEMA show severe aggregation even at concentration of 0.25 mg/mL.

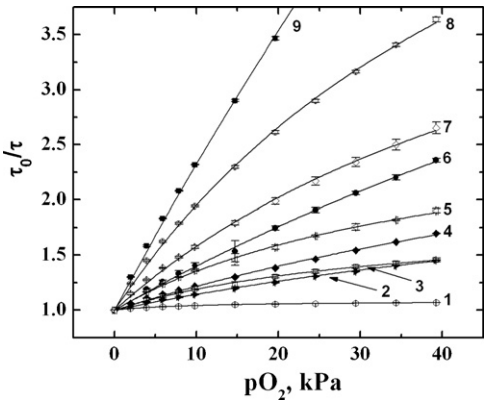

Fig. 3. Stern–Volmer plots for the $Ir(C_s)_2(acac)$ in polymeric nanobeads obtained by fast precipitation with water: (1) PViCl-PAN; (2) PMMA-MA; (3) D7; (4) PSulf; (5) D4; (6) H15; (7) RS 100; (8) RL 100; and (9) EC. The concentration of the polymer in all the cases was 0.2% (w/w) and the dye 0.002% (w/w). The decay times in the absence of oxygen (τ_0) were 16.2, 16.9, 15.2, 11.6, 13.7, 11.1, 16.5, 16.6 and 14.5 μs for (1)–(9), respectively. The non-linear fit is performed according to the "two-site" model [32].

It was found that most of the polymeric beads can be freeze dried, stored in the dry condition and redispersed in water. However, in most cases the size of the beads increases significantly after they are redispersed and exceeds 100 nm. Still, the beads stained with luminescent indicators fully retain their sensing properties. Generally, the strongly charged beads are the best dispersible after freeze-drying. Unfortunately, the beads making use of hydrogels were found not to be redispersible.

3.3. Examples of optical nanosensors

In the following we will demonstrate application of the beads for optical sensing of several important analytes such as oxygen, pH, NH_3, CO_2, and Cl^-.

3.3.1. Nanobeads for oxygen sensing

The iridium(III) coumarin complex $Ir(C_S)_2(acac)$ was chosen to probe the sensitivity of the beads. This phosphorescent indicator benefits from strong absorption in the visible region and high emission quantum yields [30]. We found that the indicator can be incorporated in all investigated polymers. It is important to note that the beads can also be stained with other common oxygen indicators such as ruthenium(II) polypyridyl complexes and metalloporphyrins. Fig. 3 demonstrates the Stern–Volmer plots for the oxygen-sensitive beads that make use of $Ir(C_S)_2(acac)$. The sensitivity of the beads is in good correlation with gas permeabilities of the polymers. The highest sensitivity to oxygen is observed for ethylcellulose beads ($\tau_0/\tau_{air\ sat} = 3.6$). The iridium(III) complex is virtually insensitive to oxygen if embedded in gas-blocking PViCl-PAN beads ($\tau_0/\tau_{air\ sat} = 1.056$). It was found that the PViCl-PAN beads produced via slow precipitation show even lower cross-sensitivity to oxygen ($\tau_0/\tau_{air\ sat} = 1.006$). The size of these beads is much higher ($Z_{av} = 210$ nm) so that very few dye molecules are located close to the

surface of the bead. The iridium(III) coumarin embedded into the positively charged RL-100 and RS-100 beads show relatively high sensitivity to oxygen ($\tau_0/\tau_{air\ sat}$ = 2.36 and 2.03, respectively). On the contrary, the sensitivity is rather low in case of PMMA-MA bearing negatively charged carboxy-groups. In fact, $\tau_0/\tau_{air\ sat}$ was found to be 1.27. It is evident that sensitivity of the Ir(C$_S$)$_2$(acac)/PMMA-MA nanosensors is too low for measurements at physiologically relevant conditions. However, PMMA-MA turned out to be an excellent matrix for immobilization of palladium(II) benzoporphyrin complexes. For example, palladium(II) tetraphenyltetrabenzoporphyrin is excellently compatible with the lines of He–Ne laser (632.8 nm), red laser diodes (635 nm) and a mercury lamp (436 nm line) since the excitation is located at 442 nm and 628 nm (Fig. S8, insert). Very high molar absorption coefficients (ε = 416,000 and 173,000 M^{-1} cm^{-1} at 442 and 628 nm, respectively) in combination with moderate quantum yields (QY = 0.21) [33] are responsible for excellent brightnesses (ε·QY). However, potential application of the indicator in microscopy and for confocal imaging is compromised by too high sensitivity in most polymers including those based on polystyrene (such as PS-MA or PS-PVP). As can bee seen (Fig. S8), the indicator is excellently suitable for measurements at 0–100% air saturation if embedded in PMMA-MA ($\tau_0/\tau_{air\ sat}$ = 3.64). Therefore, these small and stable nanobeads can be considered as an alternative to red light-excitable water-soluble dendrimeric benzoporphyrins [34].

As we demonstrated above, the size of the nanobeads can depend on several parameters including speed of precipitation, polymer concentration and composition of the solvents. It is interesting to compare the sensing properties of the nanobeads that make use of the same materials (indicator and polymer) but are obtained via different techniques. Fig. 4 shows Stern–Volmer plots for the Ir(C$_S$)$_2$(acac) embedded in PS-MA beads. The beads obtained via slow precipitation (Z_{av} 360 nm) behave very similarly to the bulk PS-MA film optode. However, beads obtained via fast precipitation from THF show increased sensitivity to oxygen and longer decay times. Interestingly, the decay times increase even further if precipitation is performed from THF:acetone mixtures. Higher amount of acetone in case of PS-MA favors longer decay times and higher sensitivities to oxygen. Notably, the size of the beads does not decrease significantly (Table 1). The higher degree of non-linearity is also evident for the beads obtained via precipitation from THF:acetone mixtures. In a good agreement with the so-called "two-site" model

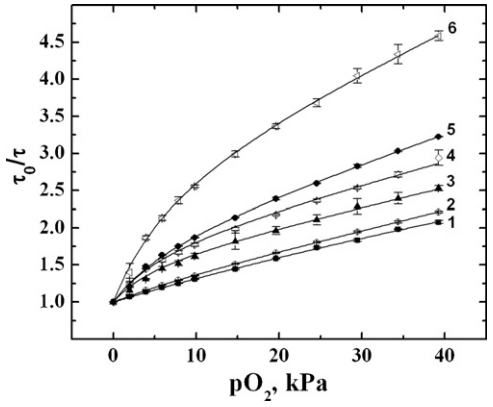

Fig. 4. Stern–Volmer plots for the Ir(C$_S$)$_2$(acac) in PS-MA bulk optode (1) and for the same indicator in PS-MA beads obtained by precipitation with water: (2) slow addition into THF solution; (3) fast addition into THF solution; (4) fast addition into the solution in THF:acetone (3:1); (5) fast addition into the solution in THF:acetone (1:1); and (6) fast addition into the solution in THF:acetone (1:7). The concentration of the polymer in all the cases was 0.2% (w/w) and the dye 0.002% (w/w). The decay times in the absence of oxygen (τ_0) were 10.6, 11.0, 12.6, 13.4, 13.6 and 15.0 μs for (1)–(6), respectively. The non-linear fit is performed according to the "two-site" model [32].

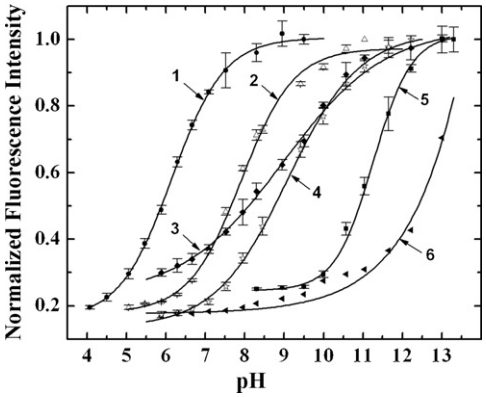

Fig. 5. Calibration plots for the pH-sensitive nanobeads based on FODE (IS = 0.05 M): (1) RL 100; (2) D4; (3) PS-MA; (4) H15; (5) PMMA-MA; (6) EC.

[35] the indicator is likely to be localized in two different environments. The quenching constants and decay times are significantly different for both environments. A fit indicates that contribution of the more quenchable fraction increases at higher amount of acetone in the "cocktail". We have found that the same trend is valid if other oxygen indicators are used. For example, the decay times in the absence of oxygen were found to be 65 and 69 μs, and τ_0/τ values were 2.49 and 3.44, for the beads stained with PtTFPP from THF and THF:acetone (1:7), respectively.

3.3.2. Nanobeads for sensing pH

A lipophilic pH indicator fluorescein octadecylester (FE) was utilized to render the nanobeads pH-sensitive. The calibration curves are shown in Fig. 5. As expected, the pK_a is much lower in positively charged RL-100 and RS-100 beads (6.2 and 6.3, respectively) than in negatively charged PS-MA and PMMA-MA particles (9.1 and 11.2, respectively). The pK_a values of 7.9 and 8.0 are observed in neutral beads of hydrogel D4 and D7, but increase significantly in more hydrophobic H 15 (pK_a = 9.1). Finally, FE embedded in even more hydrophobic ethylcellulose shows little dependence up to pH ~11, and the pK_a is very high (~13.5). As can be seen, the titration curve in case of the PS-MA beads is very wide. This effect is likely to originate from localization of the indicator in regions of varying polarity where the pK_a values of individual dye molecules are rather different. Such interesting behavior can be made use of to design the nanosensors operating in a very broad pH range. It should be mentioned that a variety of lipophilic pH indicators are available, including for example those based on fluoresceins [29] and 8-hydroxy-1,3,6-pyrenetrisulfonate (HPTS) [36,37]. These indicators can be embedded into the beads to design nanosensors operating in significantly different pH ranges. For example, a photostable 2′,7′-dichlorofluorescein octadecylester (DCFODE) seems to be a very promising candidate here since the pK_a is known to be significantly lower than for FODE [29]. Thus, the nanosensors based on DCFODE embedded in PS-MA and H15 are expected to work in physiologically relevant range (pK_a ~7.0).

3.3.3. Nanobeads for optical temperature sensing and for DLR-referencing

Optical sensors for oxygen, carbon dioxide, ammonia and many other analytes are known to show non-negligible (and often rather pronounced) cross-sensitivity to temperature. That is also the case with optical nanochemosensors. Beads which are capable of optically monitoring temperature can be dispersed together with other nanosensors to compensate them for temperature effects. Recently, we reported several temperature probes based on luminescent europium(III) complexes incorporated into bulk polymer matrices [32]. We discovered that it is also possible to prepare

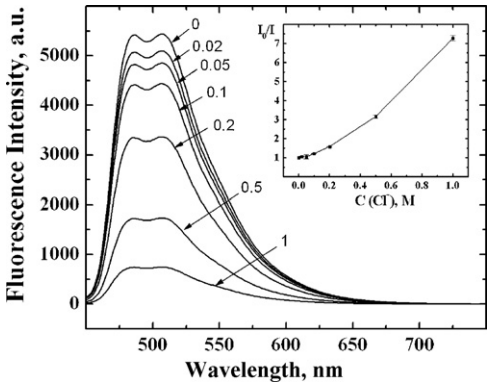

Fig. 6. Quenching of the fluorescence of lucigenin embedded into Nafion® beads by chloride ions (in M). The insert shows a corresponding Stern–Volmer plot.

temperature nanosensors via precipitation methods. For example, a europium(III) complex can be easily incorporated into a gas-blocking PViCl-PAN beads. The beads obtained via slow precipitation show negligible cross-sensitivity to oxygen. At the same time, the luminescence decay time is highly temperature-dependent (Fig. S9) and the temperature coefficient approaches 1%/K.

Recently we demonstrated that $Ir(C_S)_2(acac)$ embedded into oxygen-impermeable PViCl-PAN microparticles can be a very promising material for DLR (=dual lifetime referencing) [38]. In order to be suitable for referencing, the beads should be insensitive to the analyte of interest (e.g. CO_2 or NH_3) but also to oxygen, and preferably show low temperature sensitivity. The beads should also be small enough to form a homogeneous sensor layer after mixing with analyte-sensitive beads. Thus, the $Ir(C_S)_2(acac)$/PViCl-PAN beads obtained via slow precipitation are particularly promising here. In fact, the particles show virtually no cross-sensitivity to oxygen and very low temperature dependence of the decay time (Fig. S9).

3.3.4. Nanobeads for determination of salinity

Huber et al. reported earlier the optical salinity sensors based on Nafion® cation exchange membrane [39]. The chloride-sensitive indicator lucigenin was irreversibly electrostatically absorbed on the membrane and its fluorescence was dynamically quenched in presence of chloride ions. We found that nanoparticles for determination of salinity can be prepared via precipitation. Indeed, the particles are nicely suitable for determination of salinity in the range from 0.02 to 1 M (Fig. 6). It is likely that apart from dynamic quenching, some static quenching also takes place since the Stern–Volmer intensity plot curves upwards. Comparison to the literature data [39] indicates that the sensitivity of the beads is very close to that of the bulk optode. As was recently demonstrated by Bychkova and Shvarev [40], the precipitation method can also be used for preparation of other ion-sensitive nanobeads such as those for Na^+, K^+ and Ca^{2+}.

3.3.5. Nanobeads for sensing acidic and basic gases

Apart from oxygen, carbon dioxide and ammonia belong to the most important gaseous analytes. In contrast to oxygen, optical sensors for CO_2 and NH_3 rely on the use of pH indicators as transducers. Thus, a protective hydrophobic layer is essential to avoid cross-sensitivities to pH and ions. This makes the design of water-dispersible nanosensors an extremely challenging task. However, the nanobeads can be used in bulk optodes if immobilized in a gas-permeable hydrophobic (e.g. silicone) layer. We found precipitation to be a very useful method for the preparation of such nanobeads. For example, beads making use of ethylcellulose, HPTS and a lipophilic organic base tetraoctylammonium hydroxide TOAOH (so-called Mills-type optode) [41] can be obtained via precipitation with water. The indicator (HPTS) is extracted into the polymer in form of a lipophilic ion pair with TOA. The freeze-dried beads dispersed in silicone were found to be nicely suitable for the determination of carbon dioxide with the sensitivity similar to that of a bulk optode.

Similarly to the CO_2-sensitive beads, fluorescent nanobeads for NH_3 can be obtained via precipitation. Again, the beads are hardly suitable for sensing in aqueous media because of the cross-talk to pH. However, these beads were found to be very useful for designing optodes for trace ammonia sensing. The sensor membranes typically contain the NH_3-sensitive nanobeads dispersed in silicone, as was previously described in more detail [27]. An additional ~1 μm silicone layer is added to increase the robustness of the sensor. Fig. 7 shows the calibration plots for the sensor membranes making use of DCFME embedded in various cellulose ester nanobeads. It is evident that the sensitivity of the material can be tuned by choosing the appropriate polymer. The highest sensitivities (and the lowest limits of detection) were found for the beads making use of cellulose acetate and cellulose acetate propionate, while less sensitive sensors were obtained in case of cellulose acetate butyrate. These sensor materials were found to exhibit a 50% signal change at 117, 133 and 1909 $\mu g\,L^{-1}$ of NH_3, respectively. For comparison, a bulk optode (DCFME dissolved in cellulose acetate) is much less sensitive to ammonia (50% signal change at 2290 $\mu g\,L^{-1}$). Although such a high sensitivity of the beads cannot be fully understood, it is likely to originate from localization of the dye molecules on the surface of the nanospheres. It should be mentioned that the nanobeads are not only promising for designing ultra-sensitive ammonia sensors but also simplify the preparation of referenced sensing materials [38].

3.3.6. Nanosensors with enhanced brightness

Recently we presented a versatile method of enhancing sensor brightness by means of light-harvesting [42]. Addition of fluorescent antenna (that efficiently collects light in a desired part of the spectrum) to an indicator was demonstrated to result in dramatical increase in brightness. This simple method (requiring no synthetic modifications) was found to be very useful for oxygen, pH and other sensors. We discovered that this methodology can also be used to obtain brighter beads via precipitation. As an example, Fig. 8 shows the excitation and the emission spectra of the PMMA-MA nanobeads stained both with a coumarin antenna C 545T and with an oxygen indicator PtTFPP. Efficient excitation from 450 to 470 nm becomes possible where especially bright blue LEDs are available. Direct excitation in the Q-bands of the platinum(II) porphyrin is much less efficient (Fig. 8a) while excitation by the UV light in

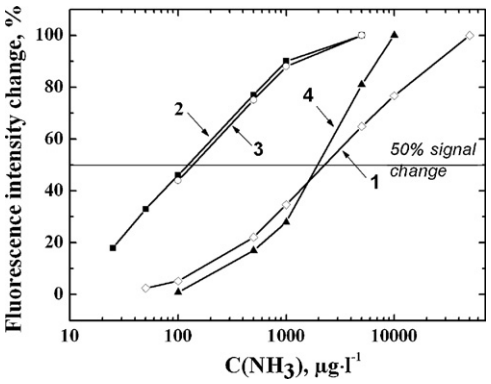

Fig. 7. Calibration plots for NH_3-sensing materials based on dichlorofluorescein methylester contained in cellulose acetate layer (1) and embedded into cellulose ester nanoparticles:cellulose acetate (2), cellulose acetate propionate (3) and cellulose acetate butyrate (4).

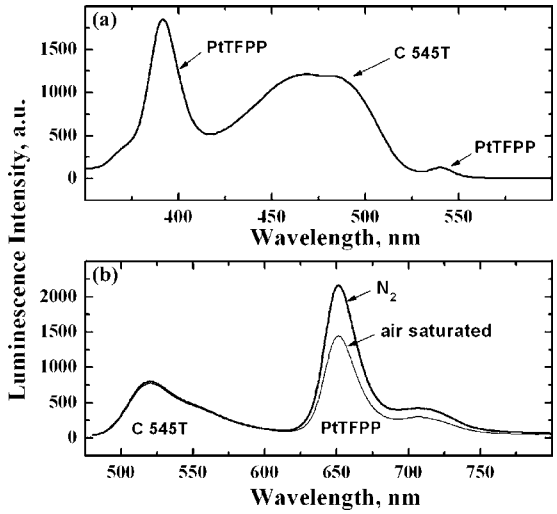

Fig. 8. Spectral properties of the PMMA-MA nanobeads stained with 2% (w/w) of the RET donor C 545T and 1% (w/w) of the RET acceptor PtTFPP: (a) excitation spectrum (λ_{em} = 650 nm); (b) emission spectra of the air-saturated and oxygen-free dispersion (λ_{exc} = 470 nm).

the Soret band is undesirable for a few reasons (e.g. high level of background fluorescence). It is also evident (Fig. 8b) that the beads are nicely suitable for ratiometric oxygen imaging since the fluorescence of the coumarin (peaking at 520 nm) is independent on oxygen content. Lifetime imaging is, of course, also possible.

3.3.7. Nanosensors with magnetic properties

Recently, attention of researches was attracted to sensors with magnetic properties [43–45]. The distinguished feature of these smart tools is the possibility to be guided to the region of interest and be collected there. It was demonstrated that very few beads with magnetic properties are sufficient to generate high signals if collected with special magnetic separators [46]. As shown previously, magnetic microbeads can be prepared via different techniques (e.g. spray-drying) [47]. We found that nanosensors with magnetic properties can also be manufactured easily. As an example, Fig. 9 shows photographic images of the dispersion of the oxygen-sensitive nanobeads (Z_{av} = 186 nm, PDI 0.029) based on $Ir(C_5)_2$(acac) embedded into PS-MA via fast precipitation from THF. To render the beads magnetic, lipophilic magnetite was added to the "cocktail" and was incorporated inside during precipitation. As can be seen, the homogeneous suspension of the beads is efficiently collected with the help of a magnet (located to the left from the cuvette). Most of the beads are collected within 1 h, while several more hours are needed to collect all the beads. The magnetic adaptors for optical fibers [46] can, of course, also be used with magnetic nanosensors. It should be mentioned that the amount of magnetite in the beads is not uniform. In other words, some particles contain more magnetite and are, therefore, more magnetic, while other contain less magnetite and are more difficult to collect. Thus, prior to use, the beads were magnetically collected within a few hours and the aqueous phase was discarded so that only particles with high magnetite doping were used further.

3.3.8. Tracers and labels

Above we provided several examples of nanobeads with sensing properties that can be easily prepared via precipitation. However, the scope of this versatile method is not limited by optical nanochemosensors. It is important that also inert lipophilic dyes can be embedded into the beads in a similar manner to obtain luminescent tracers. We found out that the procedure works excellently with such dyes as coumarins and perylens. Of course, other

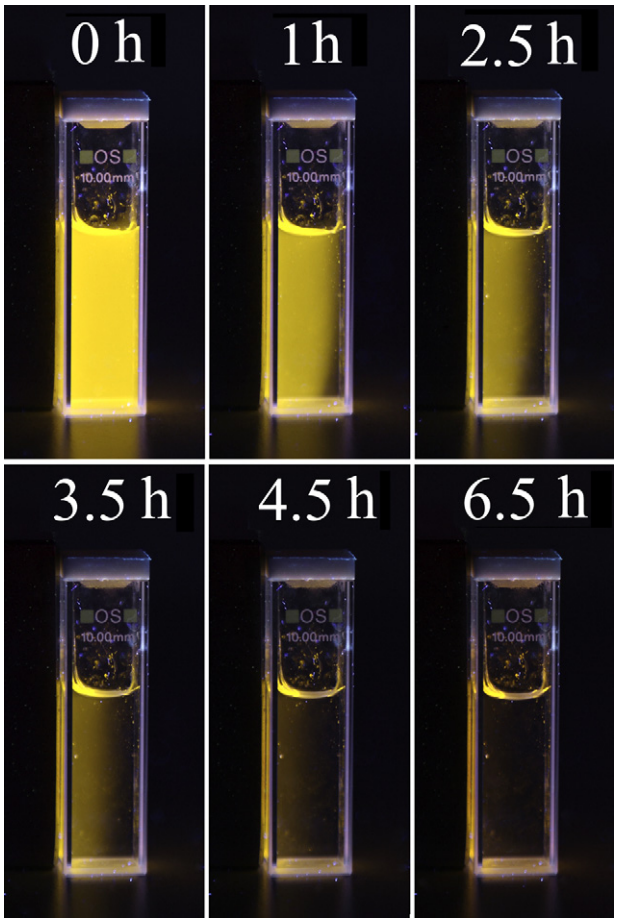

Fig. 9. Photographic images of the dispersion of magnetic oxygen nanosensors ($Ir(C_5)_2$(acac) in PS-MA) during collection phase. The magnet is located to the left from the cuvette.

dyes can be used as well. Some of the polymeric materials (such as PS-MA and especially PMMA-MA) bear carboxyl-groups which can be made use of for further functionalization and/or covalent coupling. This, in principle, enables preparation of highly luminescent labels. The size of the beads (~50 nm) is likely to be reduced further if the polymers with higher amount of carboxyl-groups (e.g. 15%) are used and precipitation is performed from more diluted solutions. It is important that both fluorescent and phosphorescent dyes (that enable time resolved measurements) can be used. In case of the latter, promising candidates include, e.g. europium(III) and terbium(III) complexes since their luminescence remains virtually independent on oxygen content. However, other classes of phosphorescent dyes such as cyclometallated complexes and metalloporpyrins can also be used providing that quenching by oxygen is not very significant [22,48]. Finally, other luminescent materials such as quantum dots or phosphors may also be embedded into the polymeric beads via precipitation.

4. Conclusions

It was demonstrated that precipitation is an extremely versatile method for producing optical nanochemosensors. This very simple technique can be used to produce large quantities of nanosensors from commercially available polymers without use of undesired additives such as surfactants. A variety of polymers and lipophilic indicators was shown to be nicely suitable for precipitation. Thus, nanosensors for oxygen, pH, temperature and salinity were obtained. Moreover, nanobeads sensitive to carbon dioxide

and ammonia can also be manufactured and used for preparation of optical sensors. The same methodology can be used for the preparation of fluorescent labels. Considering nanosensors, their sensitivity can be tuned by choosing appropriate polymer/indicator combinations. Brightness of the nanosensors can also be enhanced by making use of light harvesting. Additionally, nanosensors with magnetic properties are manufactured. These analytical tools, particularly, can be manipulated and collected in the place of interest.

Acknowledgement

The financial support by Austrian Science Fund FWF (Lise Meitner Stipendium M 1107-N22) is greatly acknowledged.

Appendix A. Supplementary data

Supplementary data associated with this article can be found, in the online version, at doi:10.1016/j.talanta.2009.05.041.

References

[1] R.N. Glud, N.B. Ramsing, J.K. Gundersen, I. Klimant, Mar. Ecol. Prog. Ser. 140 (1996) 217–226.
[2] G. Liebsch, I. Klimant, B. Frank, G. Holst, O.S. Wolfbeis, Appl. Spectrosc. 54 (2000) 548–559.
[3] T.C. O'Riordan, H. Voraberger, J.P. Kerry, D.B. Papkovsky, Anal. Chim. Acta 530 (2005) 135–141.
[4] O.S. Wolfbeis, Adv. Mater. 20 (2008) 3759–3763.
[5] B. Zelelow, G. Khalil, G. Phelan, B. Carlson, M. Gouterman, J.B. Callis, L.R. Dalton, Sens. Actuators B 96 (2003) 304–314.
[6] M. Gouterman, J. Callis, L. Dalton, G. Khalil, Y. Mebarski, K.R. Cooper, M. Greiner, Meas. Sci. Technol. 15 (2004) 1986–1994.
[7] I. Klimant, V. Meyer, M. Kuhl, Limnol. Oceanogr. 40 (1995) 1159–1165.
[8] E.J. Park, K.R. Reid, W. Tang, R.T. Kennedy, R. Kopelman, J. Mater. Chem. 15 (2005) 2913–2919.
[9] A.S. Kocincova, S.M. Borisov, Ch. Krause, O.S. Wolfbeis, Anal. Chem. 79 (2007) 8486–8493.
[10] H.A. Clark, M. Hoyer, M.A. Philbert, R. Kopelman, Anal. Chem. 71 (1999) 4831–4836.
[11] J.W. Aylott, Analyst 128 (2003) 309–312.
[12] S.M. Borisov, I. Klimant, Analyst 133 (2008) 1302–1307.
[13] M.E. Koese, B.F. Carrol, K.S. Schanze, Langmuir 21 (2005) 9121–9129.
[14] S.M. Borisov, A.S. Vasylevska, Ch. Krause, O.S. Wolfbeis, Adv. Funct. Mater. 16 (2006) 1536–1542.
[15] M.G. Sandros, V. Shete, D.E. Benson, Analyst 131 (2006) 229–235.
[16] K. Aslan, M. Wu, J.R. Lakowicz, C.D. Geddes, J. Am. Chem. Soc. 129 (2007) 1524–1525.
[17] A. Burns, P. Sengupta, T. Zedayko, B. Baird, U. Wiesner, Small 2 (2006) 723–726.
[18] V.J. Hammond, J.W. Aylott, G.M. Greenway, P. Watts, A. Webster, C. Wiles, Analyst 133 (2008) 71–75.
[19] J.P. Sumner, N.M. Westerberg, A.K. Stoddard, C.A. Fierke, R. Kopelman, Sens. Actuators B 113 (2006) 760–767.
[20] H. Sun, A.M. Scharff-Poulsen, H. Gu, K. Almdal, Chem. Mater. 18 (2006) 3381–3384.
[21] S.M. Borisov, T. Mayr, I. Klimant, Anal. Chem. 80 (2008) 573–582.
[22] J.M. Kuerner, I. Klimant, Ch. Krause, H. Preu, W. Kunz, O.S. Wolfbeis, Bioconjugate Chem. 12 (2001) 883–889.
[23] A. Pfister, G. Zhang, J. Zareno, A.F. Horwitz, C.L. Fraser, ACS Nano 2 (2008) 1252–1258.
[24] T. Higuchi, H. Yabu, M. Shimomura, Colloids Surf. A 284/285 (2006) 250–253.
[25] H. Yabu, T. Higuchi, M. Shimomura, Adv. Mater. 17 (2005) 2062–2065.
[26] G. Zhao, T. Ishizaka, H. Kasai, H. Oikawa, H. Nakanishi, Chem. Mater. 19 (2007) 1901–1905.
[27] K. Waich, T. Mayr, I. Klimant, Talanta 77 (2008) 66–72.
[28] E. Wang, G. Wang, L. Ma, C.M. Stivanello, S. Lam, H. Patel, Anal. Chim. Acta 334 (1996) 139–147.
[29] B.M. Weidgans, Ch. Krause, I. Klimant, O.S. Wolfbeis, Analyst 129 (2004) 645–650.
[30] S.M. Borisov, I. Klimant, Anal. Chem. 79 (2007) 7501–7509.
[31] O.S. Finikova, A.V. Cheprakov, I.P. Beletskaya, P.J. Carroll, S.A. Vinogradov, J. Org. Chem. 69 (2004) 522–535.
[32] S.M. Borisov, I. Klimant, J. Fluoresc. 18 (2008) 581–589.
[33] S.M. Borisov, G. Nuss, W. Haas, R. Saf, M. Schmuck, I. Klimant, J. Photochem. Photobiol. A: Chem. 201 (2009) 128–135.
[34] I. Dunphy, S.A. Vinogradov, D.F. Wilson, Anal. Biochem. 310 (2002) 191–198.
[35] L. Sacksteder, J.N. Demas, B.A. DeGraff, J.R. Bacon, Anal. Chem. 65 (1993) 3480–3483.
[36] G.J. Mohr, T. Werner, O.S. Wolfbeis, J. Fluoresc. 5 (1995) 135–138.
[37] S.M. Borisov, D.L. Herrod, I. Klimant, Sens. Actuators B 139 (2009) 52–58.
[38] K. Waich, S.M. Borisov, T. Mayr, I. Klimant, Sens. Actuators B 139 (2009) 132–138.
[39] Ch. Huber, I. Klimant, Ch. Krause, T. Werner, T. Mayr, O.S. Wolfbeis, Fresenius J. Anal. Chem. 368 (2000) 196–202.
[40] V. Bychkova, A. Shvarev, Anal. Chem. 81 (2009) 2325–2331.
[41] A. Mills, Q. Chang, Anal. Chim. Acta 285 (1994) 113–123.
[42] T. Mayr, S.M. Borisov, T. Abel, K. Waich, G. Mistlberger, I. Klimant, Anal. Chem. (2009) in press.
[43] J.N. Anker, Y.-E. Koo, R. Kopelman, Sens. Actuators B 121 (2007) 83–92.
[44] M.J. Li, Z. Chen, V.W.W. Yam, Y. Zu, ACS Nano 2 (2008) 905–912.
[45] P. Chojnacki, G. Mistlberger, I. Klimant, Angew. Chem. Int. Ed. 46 (2007) 8850–8853.
[46] G. Mistlberger, P. Chojnacki, I. Klimant, J. Phys. D: Appl. Phys. 41 (2008) 085003 (9 pp.).
[47] G. Mistlberger, S.M. Borisov, I. Klimant, Sens. Actuators B 139 (2009) 174–180.
[48] A.E. Soini, L. Seveus, N.J. Meltola, D.B. Papkovsky, E. Soini, Microsc. Res. Technol. 58 (2002) 125–131.